

Direct experimental evidence of growing dynamic length scales in confined colloidal liquids

Prasad S. Sarangapani,¹ Andrew B. Schofield,² and Yingxi Zhu^{1,*}

¹*Department of Chemical and Biomolecular Engineering, University of Notre Dame, Notre Dame, Indiana 46556, USA*

²*School of Physics, University of Edinburgh, Kings Buildings, Edinburgh EH9 3JZ, United Kingdom*

(Received 21 June 2010; revised manuscript received 3 February 2011; published 28 March 2011)

The modification of the glass transition in confined domains, particularly the length scales associated with cooperative motion, remains a mystery. Hard-sphere suspensions are confined between two surfaces to progressively smaller dimensions to probe the confinement effect on the growth of dynamic heterogeneities via confocal microscopy. The confinement length scale is defined as the critical spacing where deviations from bulk behaviors begin and is observed to occur at progressively larger gap spacings as the volume fraction is increased. However, dynamic length scales extracted from the four-point correlation function are on average smaller than the confinement length scale.

DOI: [10.1103/PhysRevE.83.030502](https://doi.org/10.1103/PhysRevE.83.030502)

PACS number(s): 64.70.pv, 68.15.+e, 83.10.Tv

Soft matter confined between surfaces or at interfaces occurs ubiquitously in nature and modern technological applications [1–3]. Despite extensive interest and activity of research in this area, major questions regarding the modification of material properties in confined domains remain. Among the myriad physical phenomena observed in confined domains, the modification of the glass transition temperature, T_g , in confinement has received the most attention yet remains contentious [4,5]. Understanding the nature of the glass transition in confinement has significant impact on many unresolved problems ranging from the instability of sub-100 nm polymer nanostructures in data storage applications to protein folding [6,7].

Interest in the confinement effect on the *dynamics* close to the glass transition was initially motivated by the desire to extract a “dynamic” length scale of molecular cooperativity, which is often masked in ensemble-averaged measures [8]. When a supercooled liquid is confined to a critical dimension where strong deviations from bulk behaviors occur, a dynamic length scale for the glass transition can be possibly obtained [9]. However, in search of this parameter, numerous experiments [4,8–16] and computer simulations [4–6] with freestanding polymer thin films as well as glass formers confined in nanopores have produced contradictory results: T_g can increase [8], decrease [4,10], or remain the same [16], depending on the nature of molecule-surface interactions.

The length scales for the onset of the confinement effect on glass forming liquids, commonly referred to as the “confinement length scale,” have also been reported in the literature [10]. Computer simulations have predicted that the confinement length scale is typically larger than the size of cooperatively rearranging regions [17], which implies that the confinement length scales are *not* representative of the length scales associated with dynamical heterogeneities. Both confinement and dynamic length scales have been extracted from experimental data [18], however, the correlation between these two length scales has not been explored experimentally.

Colloidal hard-spheres have been proven as excellent model systems to study the glass transition with the distinct advantage of facile and direct visualization using a surfet

of microscopic methods ranging from wide-field microscopy to confocal scanning microscopy [19,20]. Using confocal microscopy, direct access to dynamical heterogeneities in dense “supercooled” colloidal liquids in three-dimensions becomes possible, and this technique has been used to advance the understanding of the dynamics of bulk, glassy systems and confirmed key theories [21] and predictions from computer simulations [22] relating to the glass transition. In this paper, we extend our previous work, which has demonstrated a significant slowing down of the dynamics of hard-sphere colloidal suspensions in confinement [23], to probe the relationship between the growth of dynamical heterogeneities and the confinement length scale. Our findings reported in this paper show that the growing length scales of dynamical heterogeneities are, on average, smaller than the confinement length scale, despite both strongly depending on volume fraction.

Our model hard-sphere system consists of poly(methyl methacrylate) (PMMA) suspensions (diameter, $d = 1.288 \mu\text{m}$, polydispersity <5%), sterically stabilized and impregnated with rhodamine 6G for direct visualization via confocal microscopy [24]. The particles are suspended in dioctyl phthalate which matches the index of refraction of the particles ($n = 1.494$). Sedimentation is not observed for undisturbed samples over a period $\gg 1$ year. Volume fractions ranging from $\phi = 0.40$ to 0.57 with an uncertainty of ± 0.03 are prepared and subsequently verified using Voronoi tessellation [20]. We observe no deviations from the bulk volume fraction for the range of film thicknesses probed in our experiments [25]. A homebuilt micron-gap compression apparatus as previously described in Ref. [23] is mounted on the stage of a confocal microscope (Zeiss LSM 5 Pascal, $100\times$ objective, numerical aperture (NA) = 1.4) where thicknesses, H , are explored over a range of H/d from ≈ 78 down to ≈ 11 . Boundary induced crystallization, which would be otherwise induced between smooth walls, is prevented by coating ~ 1 to 2 disordered layers of sterically stabilized PMMA particles (polydispersity $\sim 18\%$) [26] on each confining quartz surface and subsequently sintered at $T = 110^\circ\text{C}$ for 40 min. A $10 \times 10 \text{ mm}^2$ sample well is attached to the confining surfaces using UV-curing optical adhesive (Norland 80) and injected with $\sim 200 \mu\text{L}$ of PMMA suspensions. A waiting period of at least 5 h is required for density profiles to homogenize before experiments commence,

*yzhu3@nd.edu

which is a necessary step to minimize any change in the overall volume fraction during compression, otherwise leading to the formation of “depletion layers” [23]. We systematically reduce the gap spacing between two solid surfaces using a high precision micrometer (Newport) at a rate of $2 \mu\text{m}/\text{min}$ with an interval of 10–15 min between two successive compression steps to allow the dissipation of any transient flow. At each desired film thickness, we wait a minimum of 4 h before image acquisition. Film thickness is determined solely from z -stacks with an accuracy of $\pm 0.2 \mu\text{m}$. A $30 \times 30 \times 12 \mu\text{m}^3$ volume containing ~ 3000 particles is scanned every 14 s for ~ 16 h. Three-dimensional particle centroiding algorithms [27] are subsequently employed to determine particle centers with an accuracy of $0.05 \mu\text{m}$ in the x - y plane and $0.2 \mu\text{m}$ in the z direction.

We start by examining the nature of single particle displacements in confined colloidal liquids. In both bulk and confined domains, the dynamics of colloidal liquids close to the glass transition become increasingly intermittent and the rearrangements of particles are cooperative. Previous work on bulk molecular and colloidal liquids in proximity to the glass transition has shown that the distribution of particle displacements deviates from a Gaussian on the time scales of cage rearrangements, which is related to the late β relaxation regime [20,21]. Deviations from a Gaussian are quantified in terms of the non-Gaussian parameter, α_2 , which, for a one-dimensional distribution of displacements, is defined as

$$\alpha_2 = \langle x^4 \rangle / 3(\langle x^2 \rangle)^2 - 1. \quad (1)$$

This measure is most sensitive to a subensemble of particles contributing to irreversible rearrangements in liquids [20]. For a Gaussian distribution of particle displacements $\alpha_2 \approx 0$, while $\alpha_2 > 0$ for the case where a significant fraction of particles undergo larger-than-average displacements. We have examined α_2 in the x , y , and z directions for confined PMMA colloidal suspensions; however, we only show the results for particle motions parallel to the walls in Fig. 1, owing to poor resolution in the z direction that is inherent in confocal microscopy of dense colloidal systems. It is evident that the dynamics become more heterogeneous as thickness is reduced. At any time only a small number of rare “mobile” particles contribute to the growth of the non-Gaussian parameter. It is conceivable that as the film thickness is reduced, more mobile

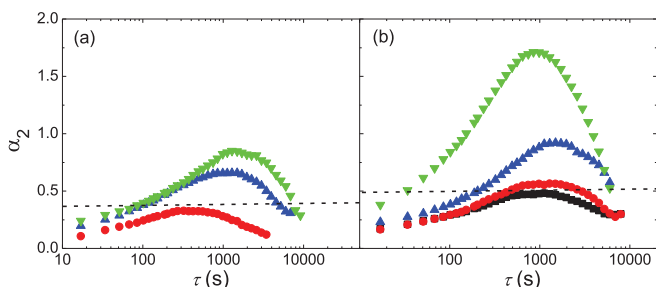


FIG. 1. (Color online) Non-Gaussian parameter α_2 measured in the x direction for $\phi =$ (a) 0.40 and (b) 0.43 at film thicknesses $H/d = 32$ (squares), 24 (circles), 15 (triangles), and 11 (inverted triangles). The horizontal dashed lines indicate the regime where deviations from bulk behavior begin to occur.

particles contribute to the tails of the probability distribution of displacements.

To further explore whether the dynamics of mobile particles is indeed facilitated, we examine the angles formed between the displacement vectors of all neighboring particles defined as $\theta = \cos^{-1}(\Delta\vec{r}_i \cdot \Delta\vec{r}_j / |\Delta\vec{r}_i| |\Delta\vec{r}_j|)$ at time scales corresponding to the peak in α_2 at varied H/d and ϕ . In Figs. 2(a)–2(c) we plot $P(\theta)$ for $\phi = 0.40$ – 0.46 . As H/d is decreased, the propensity for coherent motion of particles is greater, where at the narrowest gap, $H/d = 11$, $P(\theta)$ is strongly peaked at $\theta \approx 0$, indicating that large groups of particles move in a similar direction, as schematically illustrated in Figs. 2(d) and 2(e) for $\phi = 0.40$ and 0.43 at $H/d = 11$, respectively. It is apparent that confinement enhances the tendency of particles to move in parallel directions; such a behavior likely originates from the slow dynamics of particles immediately adjacent to the surfaces [12,28], as they are essentially caged and the slow dynamics subsequently propagate to the interior of confined colloidal film. The influence of the walls clearly becomes much stronger at narrow gaps, thereby resulting in particles exhibiting cooperative “stringlike” dynamics. This picture is qualitatively consistent with the simulation results of supercooled liquids confined in pores of controlled roughness, where the slow dynamics induced by *rough* walls may propagate to adjacent layers of the confined liquid [12] and increase the tendency of facilitated motion at narrow gaps, resulting in the enhancement of dynamic heterogeneity.

While α_2 and $P(\theta)$ show strong evidence of dynamical heterogeneity, these measures do not provide a way to measure the growing *dynamic length scales* in confinement. To find the length scales of dynamic heterogeneity associated with

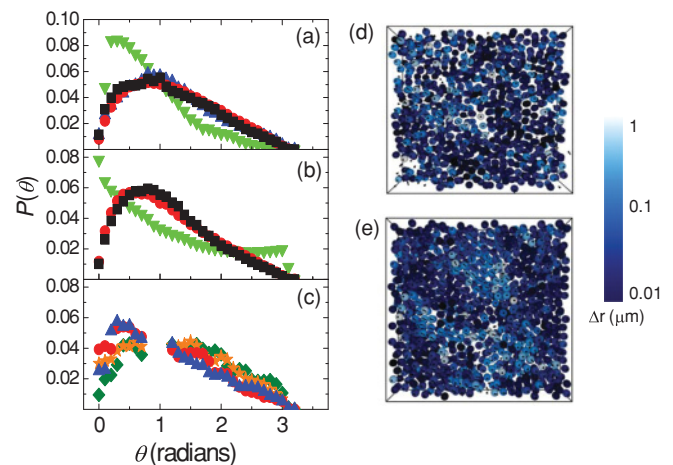


FIG. 2. (Color online) (a) Probability distribution $P(\theta)$ of angles formed between the displacement vectors of nearest neighbors at the peak time in α_2 for $\phi =$ (a) 0.40, (b) 0.43, and (c) 0.46 at $H/d = 52$ (diamonds), 40 (stars), 32 (squares), 24 (circles), 15 (triangles), and 11 (inverted triangles). In all the cases, the string-like motion, indicated by the peak of $P(\theta)$ near 0, becomes prominent as the gap is reduced, which is schematically illustrated in panels (d) and (e) for $\phi = 0.40$ and 0.43 , both at $H/d = 11$, respectively, by cutting through a three-dimensional sample $3.5 \mu\text{m}$ thick at the peak time in α_2 . Arrows indicate the direction of motion for particles with the displacement $\Delta r > 0.25 \mu\text{m}$ and have the same length in all three directions, while “dots” indicate the motion in- or out-of-plane.

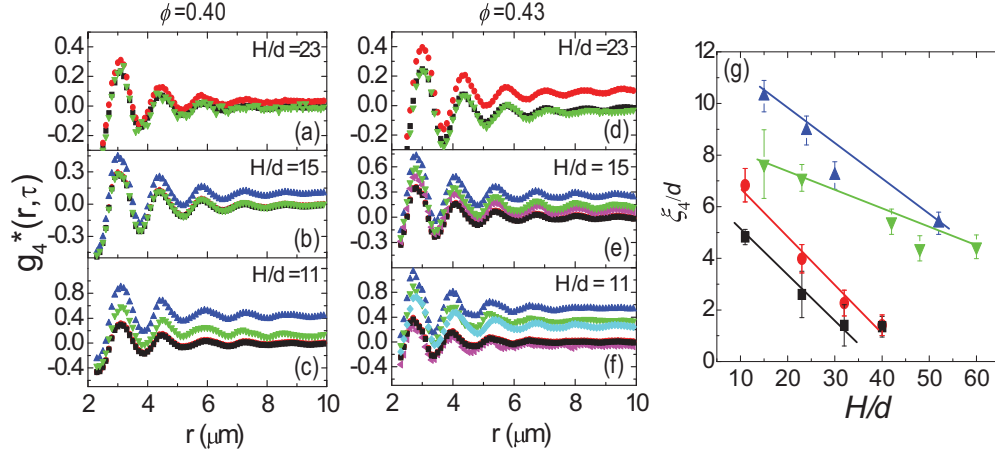


FIG. 3. (Color online) Four-point correlation function for $\phi = 0.40$ and $H/d =$ (a) 23 and $\tau = 13$ s (squares), 130 s (circles), and 1340 s (inverted triangles); (b) 15 and $\tau = 13$ s (squares), 130 s (circles), 4784 s (triangles), 7150 s (inverted triangles), and 13 560 s (left triangles); (c) 11 and $\tau = 13$ s (squares), 130 s (circles), 1340 s (inverted triangles), 4784 s (triangles), 7150 s (diamonds), and 13 560 s (left triangles); and $\phi = 0.43$ and $H/d =$ (d) 23 and $\tau = 13$ s (squares), 2600 s (circles), and 7150 s (inverted triangles); (e) 15 and (f) 11 at the same times as the ones in panels (b) and (c). (g) The length scale, ξ_4 , extracted from $g_4(r, \tau)$ close to the peak in the four-point correlation function using Eq. (3) over the range of $2 \mu\text{m} \leq r \leq 9 \mu\text{m}$ for $\phi = 0.40$ (squares), 0.43 (circles), 0.46 (triangles), and 0.57 (inverted triangles) is normalized by the particle diameter, d , and plotted against H/d .

confined colloidal thin films, it is necessary to determine the correlations in the dynamics at two different points in time and space by using the four-point correlation function, $g_4(r, \tau)$ [29] defined as

$$g_4(r, \tau) = \frac{1}{N\rho} \left\langle \sum_{ijkl} \delta[r + r_i(0) + r_k(0)] w(r_i(0) - r_j(\tau)) \right. \\ \left. \times w(r_k(0) - r_l(\tau)) \right\rangle - \left\langle \frac{Q(\tau)}{N} \right\rangle^2, \quad (2)$$

where the first term is a pair-correlation function for overlapping particles, $g_4^{\text{ol}}(r, \tau)$, and the second term is the squared mean overlaps, defined as $Q(\tau) = w(r_i(0) - r_j(\tau))$, where w is an overlapping function which is unity if $w(|r_i(0) - r_j(\tau)|)$, $w(|r_k(0) - r_l(\tau)|) \leq a$, and zero otherwise, where a ($\approx 0.63 \mu\text{m}$) is chosen to be the radius of our PMMA particles. We find that our choice of a provides the best distinction between localized and delocalized particles in our system and ensures the reproducibility of $g_4(r, \tau)$ obtained from independent data sets. In this study, we examine $g_4^*(r, \tau) = g_4^{\text{ol}}(r, \tau) / \langle Q(\tau) / N \rangle^2 - 1$. We show $g_4^*(r, \tau)$ at varied lag times and film thickness for a suspension with $\phi = 0.40$ and 0.43 in Figs. 3(a)–3(f), it is clear that the four-point correlation function captures the dynamic heterogeneity where the range of dynamical correlations are maximal at some intermediate time and also decrease on longer time scales, which is consistent with prior studies of this measure [29].

We choose to use an “envelope fitting” method to extract dynamic length scales, ξ_4 , directly from $g_4^*(r, \tau)$ on time scales where ξ_4 is maximal [30], using the relation $g_4^*(r, \tau) = A \exp(-r/\xi_4)$ over a range of $2 \mu\text{m} \leq r \leq 9 \mu\text{m}$, where A is a freely floating constant. This fitting procedure has been demonstrated to be successful in simulated supercooled liquids [29,31]. As shown in Fig. 3(g), it is clear that ξ_4 for $\phi = 0.40$ and 0.43 grows precipitously as H/d is reduced. However,

as ϕ increases toward $\phi = 0.58$ for the bulk colloidal glass transition, the effect of confinement on dynamic length scales appears much weaker. It should be noted that upon examining all the data across varied ϕ , there is indeed an apparent drop in dynamical heterogeneities when the bulk colloidal glass transition at $\phi = 0.58$ is approached, reflecting the competition between increasingly constrained dynamics at high volume fractions and dynamical fluctuations to relax the system over large length scales [31,32].

The four-point correlation function reveals the length scales associated with *dynamical heterogeneities*. However, it is also of great interest to examine the ϕ dependence on the critical dimension where spatial confinement has an effect on dynamics, thereby yielding an additional length scale for the glass transition, designated as the confinement

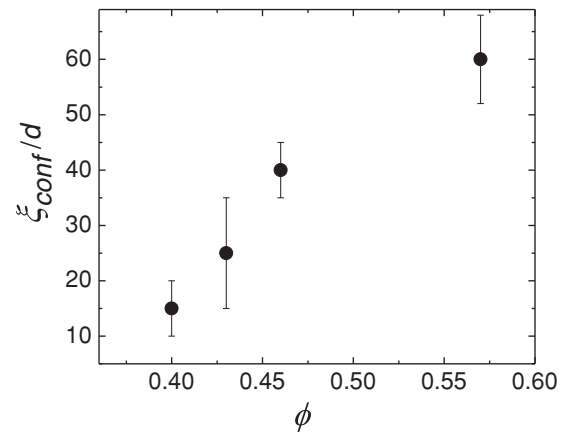


FIG. 4. Confinement length scales extracted from mean square displacement, non-Gaussian parameter as well as the four-point susceptibility at varied ϕ . Error bars indicate dispersion in thicknesses where the confinement effect begins in several independent experiments.

length scale, ξ_{conf} . To extract ξ_{conf} , we examine the H/d dependence on mean square displacements (see supplementary material—Fig. 2), four-point susceptibility (see supplementary material—Fig. 3), and α_2 for varied ϕ and pool the results to examine if there is a critical confinement length scale common to all of our measures as well as independent data sets. We define the confinement length scale as the critical thickness where deviations from bulk behavior begin to occur in all the measures examined in this study, represented as a dashed line in Fig. 1 as well as supplementary material Figs. 2 and 3. Indeed, we do find the ϕ -dependent ξ_{conf} as shown in Fig. 4. Simulations [17] have found that the length scales for dynamical heterogeneities are significantly smaller than the confinement length scale [19], which is also found to be the case for all the samples we have investigated in this work. Our results indicate that confinement results in a decrease in ϕ_g , which is analogous to an increase in T_g in the case of molecular liquids. To check our conjecture we rescale the four-point susceptibilities and investigate whether there is indeed a density-thickness superposition principle. Indeed, upon rescaling the four-point susceptibilities of confined PMMA of varied ϕ with respect to a bulk suspension of $\phi = 0.40$, we find that all the data at varied ϕ can be collapsed into a single master curve (see supplemental material—Fig. 4);

as a result, a plot of the shift factors against relative thickness is obtained to clearly indicate that ϕ_g decreases in confinement.

In summary, we have demonstrated that confinement has a strong influence on dynamics: Confined colloidal hard-spheres show a significant reduction in ϕ_g , which is accompanied by a marked increase in cooperative dynamics in confinement as the gap spacing becomes smaller than the confinement length scale. However, the effect of confinement on dynamics becomes weaker for higher ϕ as evidenced by the film thickness dependence on the dynamic length scales for $\phi = 0.46$ and 0.57 where an apparent drop in dynamic heterogeneity is observed at $\phi = 0.57$. Significantly, dynamic length scales extracted from the four-point correlation functions are on average smaller than the confinement length scale, despite both strongly depending on volume fraction. It could be interesting to further explore the relationship between structure and dynamics for binary colloidal suspensions under confinement. The shapes of rearranging regions observed in Ref. [33] for binary hard-sphere suspensions may be a consequence of changes in local structure as well.

P.S.S. and Y.Z. are grateful for financial support from the National Science Foundation under Grants No. CBET-0730813 and No. CMMI-100429.

-
- [1] S. Granick, *Phys. Today* **52**, 26 (1999).
 [2] Y. Ding *et al.*, *ACS Nano* **1**, 84 (2007).
 [3] G. Y. Jung *et al.*, *Nano Lett.* **4**, 1225 (2004).
 [4] C. L. Jackson and G. B. McKenna, *J. Non-Cryst. Solids* **131**, 221 (1991).
 [5] M. Alcoutalbi and G. B. McKenna, *J. Phys. Condens. Matter* **17**, R461 (2005).
 [6] K. V. Workum and J. J. de Pablo, *Nano Lett.* **3**, 1405 (2003).
 [7] H.-X. Zhou, G. Rivas, and A. P. Minton, *Annu. Rev. Biophys.* **37**, 375 (2008).
 [8] R. Richert, *Phys. Rev. B* **54**, 15762 (1996).
 [9] G. B. McKenna, *Eur. Phys. J. E* **12**, 191 (2003).
 [10] C. J. Ellison and J. M. Torkelson, *Nat. Mater.* **2**, 695 (2003).
 [11] F. Varnik, J. Baschnagel, and K. Binder, *Phys. Rev. E* **65**, 021507 (2002).
 [12] J. Baschnagel and F. Varnik, *J. Phys.: Condens. Matter* **17**, R851 (2005).
 [13] C. Bennemann, J. Baschangel, and W. Paul, *Eur. Phys. J. B* **10**, 323 (1999).
 [14] R. A. Riggelman, K. Yoshimoto, J. F. Douglas, and J. J. de Pablo, *Phys. Rev. Lett.* **97**, 045502 (2006).
 [15] P. P. Simon and H. J. Ploehn, *J. Rheol.* **44**, 169 (2000).
 [16] C. B. Roth, K. L. McNerny, W. F. Jager, and J. M. Torkelson, *Macromolecules* **40**, 2568 (2007).
 [17] P. Scheidler, W. Kob, and K. Binder, *J. Phys. Chem. B* **108**, 6673 (2004).
 [18] E. Donth, *The Glass Transition: Relaxation Dynamics in Liquids and Disordered Materials* (Springer-Verlag Berlin Heidelberg, 2000).
 [19] A. H. Marcus, J. Schofield, and S. A. Rice, *Phys. Rev. E* **60**, 5725 (1999).
 [20] E. R. Weeks and D. A. Weitz, *Phys. Rev. Lett.* **89**, 095704 (2002); F. P. Preparata and M. I. Shamos, *Computational Geometry* (Springer-Verlag, New York, 1985).
 [21] G. Adam and J. H. Gibbs, *J. Chem. Phys.* **43**, 139 (1965).
 [22] M. Vogel and S. C. Glotzer, *Phys. Rev. Lett.* **92**, 255901 (2004).
 [23] P. S. Sarangapani, Y. Yu, J. Zhao, and Y. Zhu, *Phys. Rev. E* **77**, 061406 (2008).
 [24] A. D. Dinsmore *et al.*, *Appl. Opt.* **40**, 4152 (2001).
 [25] See supplemental material at [<http://link.aps.org/supplemental/10.1103/PhysRevE.83.030502>] for the detailed experimental procedure.
 [26] H. Hu and R. Larson, *Langmuir* **20**, 7436 (2004).
 [27] J. C. Crocker and D. G. Grier, *J. Colloid Interface Sci.* **179**, 298 (1996).
 [28] V. N. Michailidou, G. Petekidis, J. W. Swan, and J. F. Brady, *Phys. Rev. Lett.* **102**, 068302 (2009).
 [29] N. Lacevic, F. W. Starr, T. B. Schröder, and S. C. Glotzer, *J. Chem. Phys.* **119**, 7372 (2003).
 [30] We determine the time scale at which ξ_4 is maximal by plotting ξ_4 vs τ for varied volume fraction and thickness (see supplemental material—Fig. 5), which shows that ξ_4 is small on short time scales, peaks at intermediate time scales, and decreases at long times.
 [31] P. Ballesta, A. Duri, and L. Cipelletti, *Nat. Phys.* **4**, 550 (2008).
 [32] L. Berthier, G. Biroli, J. P. Bouchaud, L. Cipelletti, D. El Masri, D. L'Hôte, F. Ladieu, and M. Pierno, *Science* **310**, 1797 (2005).
 [33] K. V. Edmond, C. R. Nugent, and E. R. Weeks, e-print [arXiv:1003.0856](https://arxiv.org/abs/1003.0856).